Site Soil Classification Interpretation Based on Standard Penetration Test and Shear Wave Velocity Data

by Windu Partono

Submission date: 10-Feb-2022 03:26PM (UTC+0700)
Submission ID: 1759165040
File name: Site_Soil_Classification_Interpretation_Based_on_Standard.pdf (1.62M)
Word count: 4215
Character count: 22221

J. Eng. Technol. Sci., Vol. 53, No. 2, 2021, 210206

Site Soil Classification Interpretation Based on Standard Penetration Test and Shear Wave Velocity Data

Windu Partono[1*], Muhammad Asrurifak[2], Edy Tonnizam[3], Frida Kistiani[1], Undayani Cita Sari[1] & Kukuh Cahya Adi Putra[1]

[1]Civil Engineering Department, Engineering Faculty, Diponegoro University, Jalan Prof. Soedarto SH., Tembalang, Semarang 50275, Indonesia
[2]Faculty of Civil Engineering and Planning, Institut Sains dan Teknologi Nasional, Jalan Moh. Kaffi II, Srenseng Sawah, Jagakarsa, Jakarta Selatan12640, Indonesia
[3]Centre of Tropical Geoengineering, Faculty of Civil Engineering, Universiti Teknologi Malaysia, 81310 UTM Johor Baru, Johor, Malaysia
*E-mail: windu_bapake_dila@yahoo.com

Highlights:

- Site soil classification was conducted using the standard penetration test (N-SPT) pressure and shear wave velocity (V_S) values.
- The V_S data were collected from single and array microtremor investigations.
- Site soil classification was calculated based on the SNI 1726:2019 seismic code.
- N-SPT maximum 120 produced different V_S and site soil classification compared to N-SPT maximum 60.

Abstract. Site soil classification provides vital information for predicting the soil amplification or the site factor. The site factor is important for calculating the surface spectral acceleration in the seismic design of buildings. Based on the Indonesian seismic code, site soil classification can be conducted by calculating the average standard penetration (N-SPT) resistance, the average shear wave velocity (V_S) and the average undrained soil strength (S_u) of the upper 30 m of a subsoil layer. Different results may be obtained at the same location when the site soil classification is predicted using N-SPT than when using V_S data. The restriction of N-SPT values until a maximum of 60 compared to a V_S maximum of 750 m/sec can produce different soil classes and will directly impact the calculation of the surface spectral acceleration. This paper describes the different results of site soil classification prediction calculated using the average N-SPT and the average V_S, conducted at Semarang City, Indonesia. Site soil classification maps developed based on both datasets are also presented, to evaluate the different site soil classification distributions. Only soil classes SD and SE were observed using N-SPT maximum 60, whereas soil classes SC, SD and SE were observed using N-SPT maximum 120.

Keywords: *bedrock; shear wave velocity; site factor; site soil classification; spectral acceleration; standard penetration pressure*.

Received May 19th, 2020, 1st Revision August 22nd, 2020, 2nd Revision October 8th, 2020, Accepted for publication November 19th, 2020.
 ISSN: 2337-5779, DOI: 10.5614/j.eng.technol.sci.2021.53.2.6

1 Introduction

The calculation of the surface spectral acceleration is important for the seismic resistance design of buildings. The Ministry of Public Works and Human Settlements [1] has created a public website facility for calculating the design spectral acceleration. The data required for design spectral acceleration calculations are building positions in terms of building coordinates (longitude and latitude) and site soil classification. Site soil classification data can be calculated either using shear wave velocity (V_S), standard penetration (N-SPT) resistance, or undrained shear strength (S_u) data [2,3]. Only three different soil classes are commonly applicable for the seismic design of buildings, namely SC (very dense soil and soft rock), SD (stiff soil) and SE (soft clay soil) [3]. N-SPT and V_S are commonly used by civil engineers in Indonesia for site soil interpretation. N-SPT values are the easiest to obtain. They are collected during soil investigations and are usually used for designing building foundations. Due to the requirements for foundation and substructure design, N-SPT data collection and acquisition are usually terminated when the N-SPT value reaches 60 (blows). When the N-SPT value exceeds 60, the N-SPT value recorded in the investigation report (boring log) is '>60', which is difficult to use for calculating site soil classes.

Other easy-to-obtain non-invasive data that can be used for site soil classification calculations are V_S data. V_S data can be observed on-site or at a building's location by performing single or array microtremor investigations. A microtremor investigation is usually performed for bedrock elevation prediction and V_S profile data acquisition from bedrock through the surface layer. Recent data are important for earthquake simulation propagation analysis or site-specific analysis. Propagation analysis is important for calculating ground motion and spectral acceleration at the earth's surface.

N-SPT and V_S data for site soil classification calculation can be developed using the average data for the top 30 m of the soil deposit and are calculated using Eqs. (1) and (2), where d_i, N_i and V_{Si} represent the thickness, the N-SPT and the shear wave velocity of a soil layer, *i*, respectively. Table 1 shows the corresponding site soil classification distribution criteria based on N_{30} and V_{S30}. Soil classes SA (Hard Rock), SB (Rock) and SF (Specific Soil) are not presented in Table 1. Average undrained shear strength data, which can also be used for site soil classification, are also not presented in this table.

$$N_{30} = \frac{\sum_{i=1}^{n} d_i}{\sum_{i=1}^{n} d_i / N_i} \tag{1}$$

$$V_{S30} = \frac{\sum_{i=1}^{n} d_i}{\sum_{i=1}^{n} d_i / v_{si}} \quad (2)$$

Table 1 Site soil classification interpretation using N_{30} and Vs_{30}.

Site Soil class	N_{30}	V_{S30} (meter/sec)
SC	>50	>350
SD	15-50	175-350
SE	<15	<175

This research presents two different results of site soil classification interpretation that were calculated using N_{30} and V_{S30} data in Semarang, Indonesia. The difference in site soil classification interpretation developed using N_{30} and V_{S30} values can produce different surface spectra accelerations. Site soil classification maps developed based on both datasets are presented to evaluate the difference soil class distributions within the research area.

2 Methodology

Site soil classification interpretation in the research area was calculated based on N-SPT and V_S datasets. The N-SPT data were collected by soil boring investigations in the study area. The minimum depth of the soil boring was 30 m, while the maximum depth was 60 m. For each boring position, the N-SPT data were collected from depths between 0 and 30 m. The V_S data investigations were performed in the research area using a 100 Hz seismometer with a maximum of 15 minutes of data recording. Three-component (south-north/SN, west-east/WE and vertical/V) ambient vibration data were collected in a single station microtremor investigation. An array microtremor investigation and analysis were also performed in the research area. Site soil classification maps were developed based on 203 soil boring points and 241 single station microtremor positions and four array microtremor investigation positions. Figure 1 shows all soil investigation (soil boring, single station microtremor, and array microtremor) positions in the research area.

2.1 Microtremor Investigation

The ambient vibration data collected using the single station and array microtremor results were analyzed using the horizontal to vertical spectrum ratio (HVSR) and inversion methods [4-7]. The purpose of HVSR analysis is to predict the bedrock elevation at the microtremor test position. The purpose of the inversion analysis is to predict the Vs profile at the microtremor test position. Figure 2(a) shows an example of the soil profile contours in terms of the V_S values

llected and analyzed using the array microtremor data from the A4 position. Figure 2(b) shows an example of the inversion analysis result of the three-component ambient vibrations developed at nine seismometer positions in the A4 array location. Figures 3(a) and (b) display the average V_S profile calculated at four different (A1-A4) array microtremor positions with a maximum depth of 30 m.

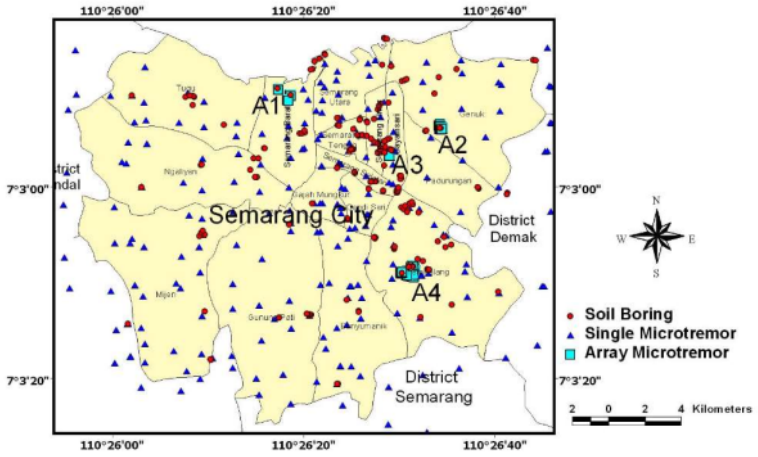

Figure 1 Soil boring and microtremor investigation positions.

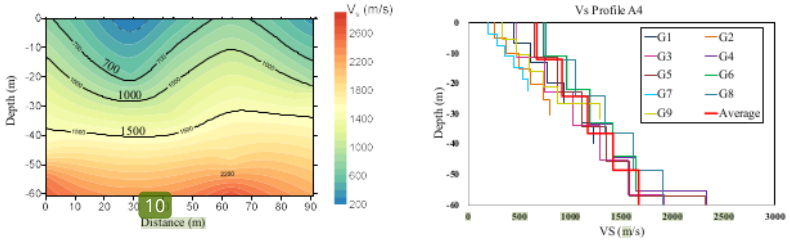

(a) (b)

Figure 2 VS contour in array A4 (a), VS profile observed in array A4 (b).

2.2 Soil Boring Investigation

Soil boring investigations were performed at 203 positions within the research area. From these 203 boring investigations, three boring investigations were conducted in array A1. Two boring investigations were performed in array A2. Two boring investigations were performed in array A3 and four boring investigations were performed in array A4. Two modified N-SPT data acquisitions were conducted at two boring positions, B191 and B199, to obtain the real N-SPT values following the same procedure as [8]. The real N-SPT values were measured when the N-SPT reached a minimum of 60. Figure 4(a) displays an example N-SPT profile with two different data format presentations. This figure was developed from one boring investigation (B191) with a maximum depth of 30 m in array position A4. The 'Reported N-SPT' within this figure represents the N-SPT value reported from the boring log, whereas the 'Real N-SPT', representing the real N-SPT, was observed during the investigation (maximum N-SPT observed is 120). Figure 4(b) shows the real N-SPT profile collected from one boring investigation (B192) in array position A1 and the maximum N-SPT observed at this position was less than 60.

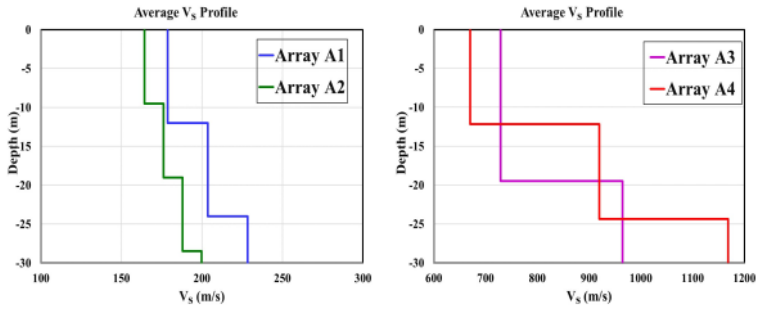

Figure 3 Average VS profile at Array 1 and 2 (a) and Array 3 and 4 (b) microtremor investigation positions.

2.3 N-SPT and V_s Correlation

N-SPT data are usually collected in soil boring investigations. V_S data can be collected from a site investigation using single station or array microtremor investigations. Another simple method for developing V_S data is by conducting laboratory investigations. The laboratory investigation for collecting V_S data was performed using undisturbed soil samples (UDS) obtained from soil boring investigations and Sonic Viewer equipment [9]. Due to the differences between the UDS diameter (±7.5 cm) and the Sonic Viewer transducer plate diameter (±

6 cm), the UDS diameter was manually reduced using a soil cutter to produce a soil sample with h ≈ 2d, where h and d are the height and diameter of the Sonic Viewer soil sample, respectively.

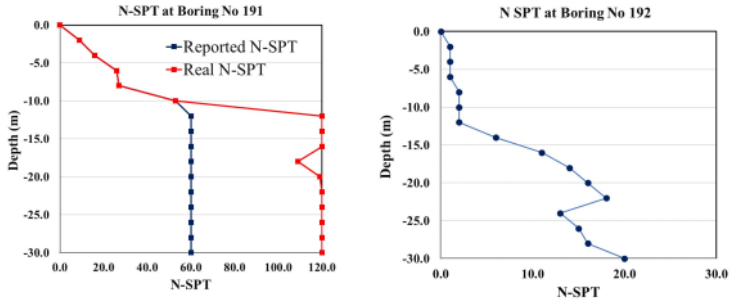

(a) (b)

Figure 4 N-SPT profile at boring No 191 in array A4 at southern region (a) and boring no. 192 in array A1 at northern region (b) of the research area.

The preliminary N-SPT and V_S correlations in the research area were developed by conducting a combination of N-SPT data and V_S laboratory data. The V_S data were observed using UDS obtained from four soil boring investigations. Table 2 shows the correlation between N-SPT and V_S conducted at four soil boring locations (9 UDS data). The N-SPT and UDS were collected at different positions within the same depth interval. The UDS were taken in between the two closest N-SPT tests (above and below the UDS position).

Table 2 Vs (laboratory investigation) and N-SPT correlation.

Sample	Depth (m)	Diameter Sample (cm)	Height Sample (cm)	Vs (m/sec)	N-SPT
lok93Bh1	7 - 8	6.00	13.00	409	30
lok99Bh1	13 - 14	5.93	11.64	393	40
lok99Bh1	19 - 20	5.90	12.09	315	40
lok99Bh2	12 - 13	6.09	11.73	458	41
lok99Bh2	16 - 17	6.21	12.02	436	35
lok92Bh1	29 - 30	5.90	12.40	488	60
lok95Bh1	17 - 18	5.95	12.94	395	40
lok95Bh1	24 - 25	5.99	13.50	489	34
lok95Bh1	28 - 29	6.02	13.13	453	35

The N-SPT value displayed in this table is the average of two N-SPT values. Due to the problem of preparing soft soil samples with an N-SPT of less than 20, the minimum N-SPT value obtained from four boring locations was 30. Figure 5 shows the N-SPT and V_S distribution and correlation developed from the preliminary investigation results.

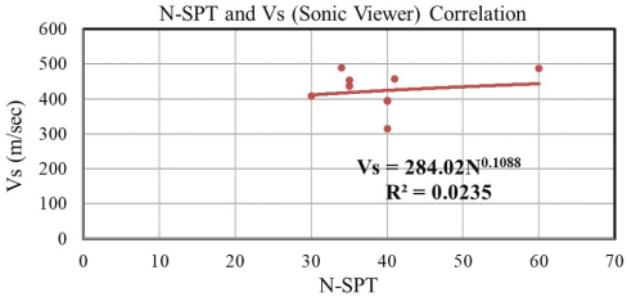

Figure 5 N-SPT and V_S (laboratory investigation) correlation.

An N-SPT and V_S correlation analysis was also performed based on two field investigations. The V_S data were collected from single station and array microtremor investigations. Due to different soil thickness intervals, all V_S profiles developed from the microtremor investigations were then linearly interpolated, following the same depth interval used by the N-SPT investigation. Figures 6 (a) and (b) display two examples of data acquisition at array A4 (boring no. 191) and array A1 (boring no. 192) positions, respectively. In these figures, 'V_S (original)' represents the original V_S distribution interval developed using inversion analysis of ambient vibrations and is distributed using a 12 m depth interval. The N-SPT data from the top soil layer to 30 m were distributed using a 3 m depth interval. The 'V_S (interpolated)' profile was developed using the same N-SPT interval.

The N-SPT and average V_S data at all four array locations were then re-analyzed to obtain the Vs and N-SPT correlations. Figure 7(a) shows the power regression results of Vs (microtremor investigation) and the N-SPT correlation curves developed in this research. The laboratory correlation was slightly higher compared to the microtremor correlation. Figure 7(b) shows the new Vs and N-SPT correlations developed in this research and compares it to five other Vs and N-SPT correlations curves from [10-14]. Similar Vs and N-SPT empirical correlations [10-12] were also used in [15] for seismic microzonation of the research area.

As can be seen in Figure 7(b), for N-SPT less than 15 the related V_S values developed from this research were slightly higher compared to the empirical correlations developed by four other researchers [10-13]. However, the opposite was observed in this research when the N-SPT value was greater than 15; the Vs value calculated using this formula was lower compared to the empirical correlations developed in Refs. [10-13]. The Vs and N-SPT correlation developed in this research was higher compared to [14].

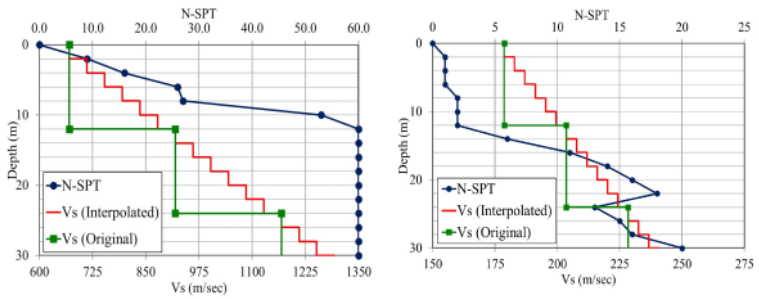

Figure 6 N-SPT and Vs interpretation at boring no. 191 (a) and no. 192 (b).

2.4 Site Soil Maps Distribution

Site soil distribution maps were developed based on three different data sets. The first site soil map was developed using the N_{30} data calculated for 203 boring positions. The second site soil map was developed using V_{S30} data calculated from an average of three empirical Vs and N-SPT correlation (Model 1) developed by [10-12]. The third site soil map was developed based on the empirical Vs and N-SPT correlation developed in this research (Model 2).

Figure 7(c) shows Models 1 and 2 correlation charts used for the development of the maps. These two models were developed from 80 data for all soil types. The two different maximum N-SPT values used in this research were 60 (N-SPT60), which was obtained from the N-SPT value reported from the boring log, and 120 (N-SPT120), based on the modified N-SPT value investigation. The N-SPT values (N-SPT120) were improved for all boring locations when the N-SPT values reported within the boring log was reported greater than 60 ('>60').

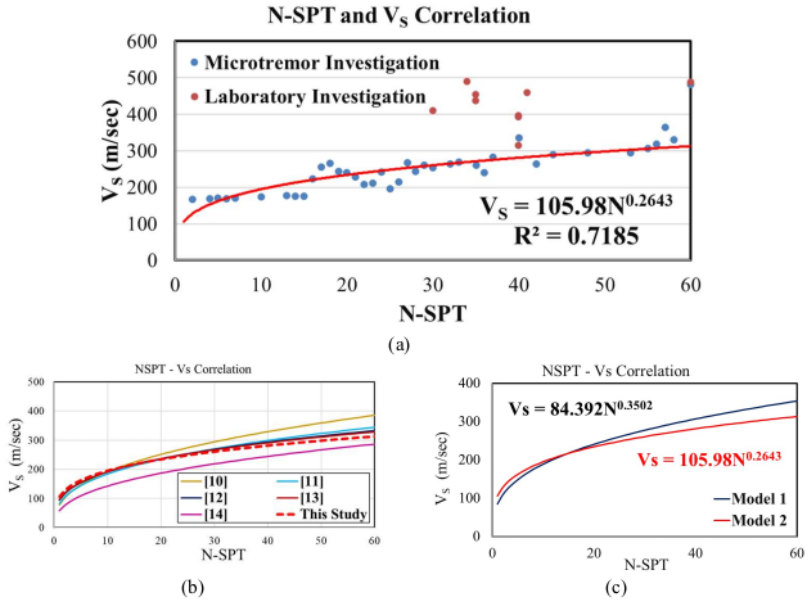

Figure 7 N-SPT and Vs correlation for all soils developed in this research (a), comparison with five other studies (b) and Model 1 and Model 2 correlations (c).

3 Results and Discussion

The site soil class distribution maps developed in this research were divided into two different datasets, N_{30} and V_{S30}. The first data set used for site soil class distribution was N_{30}. The two different approaches for N_{30} calculation are related to the N-SPT60 and N-SPT120 values used for the N_{30} calculation. Figure 8(a) shows the site soil class distribution map developed using N-SPT60 and the second map, Figure 8(b), shows the site soil class distribution based on the N-SPT120 value. As can be seen in these two figures, the distributions of the SE (soft clay soil) class are almost equal and are distributed in the northern region of the research area. The SC and SD site soil class distributions inside these two figures are quite different.

Based on the N-SPT60 values, most of the southern and middle regions of the research area are dominated by the SD soil class. The SC soil class was observed in a small area in the southern region of the research area. The SD and SE soil classes dominate the site soil classification distribution within the research area. Using the N-SPT120 values, as can be seen in Figure 8(b), the SD and SC site

soil classes were detected in the middle and southern regions of the research area. The SC area identified using N-SPT60 is smaller than the same class identified using N-SPT120. However, the SD soil class area identified using N-SPT60 is wider than the SD soil class area developed using N-SPT120.

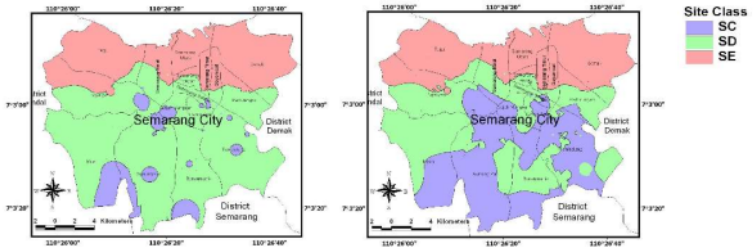

(a) (b)

Figure 8 Site soil classification maps developed using N-SPT60 (a) and N-SPT120 (b).

The second method for developing a site soil classification distribution map was performed using the V_{S30} value. The V_{S30} values developed in this method were calculated using the N-SPT60 values (maximum 60 for N-SPT value). Two different models were produced using this method. Model 1 used the NSPT (N-SPT60) and V_S empirical correlation function developed in [10-12]. Model2 used the N-SPT and V_S empirical correlation established is this research, as displayed in Figure 7(a).

Figure 9(a) shows the site soil class distribution map developed using Model 1. Figure 9(b) shows the site soil class distribution map using Model 2. As can be observed from both figures soil classes SD and SE dominate the site soil classification distribution in the research area. A small area with soil class SC was detected in the southern region of the research area when the site soil classification was developed using Model 1. Based on these figures, when the maximum N-SPT60 value was applied for site soil classification interpretation, the site soil classification distribution developed using Model 1 was almost equal to Model 2. A small area with soil class SC was observed in the research area when the site soil classification was interpolated using Model 1.

The third site soil classification distribution map was developed by applying the N-SPT120 values. Again, two different models were investigated, Models 1 and 2. The V_S values used for developing V_{S30} were calculated using the two correlation function models.

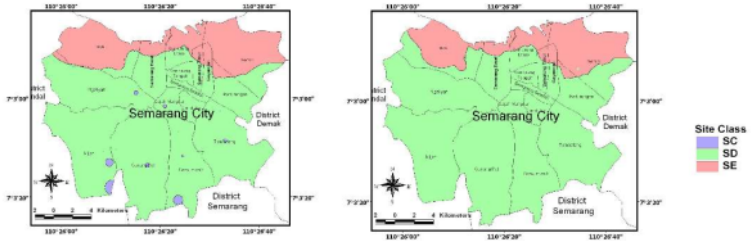

(a) (b)

Figure 9 Site soil classification maps developed using N-SPT60 values and correlation function Model 1 (a) and Model 2 (b).

Figure 10(a) presents the site soil class map developed using Model 1. Figure 10(b) presents the site soil class map developed using Model 2. Site soil classes SC, SD and SE were detected in the research area when Model 1 was applied for site soil classification calculation. However, only soil classes SD and SE were detected as major site soil classes in the research area when Model 2 was applied for the site soil classification calculation. A small SC area was detected in the southern region of the research area when Model 2 was used for site soil classification interpretation.

Based on Figures 9 and 10, soil classes SC, SD and SE were detected in the research area when N-SPT120 values and two correlation models, Model 1 and Model 2, were applied for site soil classification interpretation. However, using N-SPT60, and Model 1 and Model 2 correlations, not all soil classes were observed in the study area. When N-SPT60 was applied to Model 1 and Model 2, no soil class SC or only a small area with soil class SC was observed in the study area. Based on Figure 8(a), Figure 9 and Figure 10(b), by applying N-SPT60, the site soil classification interpretation was more consistent compared to N-SPT120.

A study for evaluating the compatibility of N-SPT and V_S correlations in producing site soil classifications was conducted by designing the N_{30} and V_{S30} correlation charts for Models 1 and 2 and applying the N-SPT60 and N-SPT120 values. N_{30} and V_{S30} correlations are said to be compatible when the same soil class is detected at the same boring positions using these two N_{30} and V_{S30} values. The evaluation was performed for all 203 data.

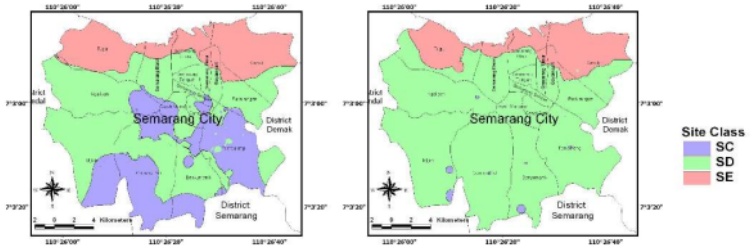

Figure 10 Site soil classification maps developed using N-SPT120 and correlation function Models 1 (a) and Model 2 (b).

Figure 11(a) shows the N_{30} and V_{S30} compatibility correlation charts using N-SPT60. Figure 11(b) shows the same compatibility correlation charts using the N-SPT120 values. The blue, green and red areas inside these two figures represent soil classes SC, SD, and SE, respectively.

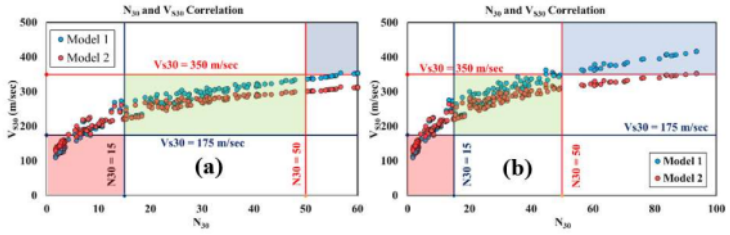

Figure 11 N_{30} and V_{S30} correlation charts developed using N-SPT60 (a) and N-SPT120 (b).

Table 3 shows the percentage distribution of soil classes SC, SD and SE observed from 203 data. The total percentage of the three classes for Model 1 and Model 2 either by using N-SPT60 or N-SPT120 was less than 100%. As can be seen in Figures 11(a) and (b) and Table 3, the N_{30} and V_{S30} correlations calculated using N-SPT60 and N-SPT120 and applying Models 1 and 2 were more compatible for all SD soil classes. The N-SPT and Vs correlation developed using Model 1 was more suitable for producing site soil classification interpretation compared to Model 2. According to Table 3, using Model 1, approximately 73% of data were compatible and 27% were not compatible in producing site soil classification interpretation. However, using Model 2, approximately 61%-66%, or average 63%, was compatible and 37% was not compatible.

Table 3 Site soil class distribution.

Model	Based on N-SPT60 (%)				Based on N-SPT120 (%)			
	SC	SD	SE	Total	SC	SD	SE	Total
Model 1	9.85	44.83	18.72	73.4	19.7	34.91	19.21	73.72
Model 2	0	44.83	16.26	61.09	7.39	42.86	15.27	65.52

4 Conclusions

Different site soil classification results are obtained when N_{30} values are applied for site soil classification interpretation than when V_{S30} values are applied. Different site soil class distribution maps are also found when the site soil classification is predicted using N_{30} and V_{S30}.

The Vs and N-SPT correlation developed using Model 1 (the average of three empirical correlations [10-12]) was slightly more consistent compared to the same correlation developed using Model 2 (based on site investigations in the research area). The site soil class distribution map developed using N-SPT60 was more consistent compared to the same map distribution developed using N-SPT120. V_{S30} calculated using N-SPT60 values was slightly less suitable for developing site soil classification compared to V_{S30} calculated using N-SPT120.

Due to the total data and undisturbed soil samples preparation used for the Vs laboratory data and the N-SPT correlation, the Vs (developed using microtremor investigation) and N-SPT correlation tests were more consistent compared to the same correlations developed using undisturbed soil samples and laboratory investigation.

Acknowledgement

This paper and the research were financially and technically supported by the Engineering Faculty, Diponegoro University, Indonesia, through Strategic Research Grant 2020.

References

[1] Ministry of Public Work and Human Settlements, *Spectral Design of Indonesia*, http://rsapuskim2019.litbang.pu.go.id/ (15 August 2020)
[2] SNI 1726:2019, *Seismic Resistance Design Codes for Building and Other Structures*, Indonesian National Standardization Agency, 2019.
[3] ASCE/SEI 7-16, *Minimum Design Loads and Associated Criteria for Buildings and Other Structures*. American Society of Civil Engineers, 2017.

[4] Fazlavi M. & Haghshenas E., *Technical Note Importance of Mode Detection in Ambient Noise Array Application for Shear Wave Velocity Profile Determination*, International Journal of Civil Engineering, **13**(1), Geotechnical Engineering, pp. 62-72, 2015.

[5] Gosar A., *Study on the Applicability of the Microtremor HVSR Method to Support Seismic Microzonation in the Town of Idrija (W Slovenia)*, Natural Hazards Earth Systems Science, **17**, pp. 925-937, 2017.

[6] Hayashi, K. & Underwood, D., *Microtremor Array Measurements and Three-component Microtremor Measurements in San Francisco Bay Area*, 15 WCEE, Lisboa, pp. 9588-9597, 2012.

[7] Koesuma, S., Ridwan, M., Nugraha, A.D., Widiyantoro S. & Fukuda, Y., *Preliminary Estimation of Engineering Bedrock Depths from Microtremor Array Measurements in Solo, Central Java, Indonesia*, Journal of Mathematics and Fundamental Science, **49**(3), pp. 306-320, 2017.

[8] Jahanger, Z.K., *Relation between Standard Penetration Test and Skin Resistance of Driven Concrete Pile in over Consolidated Clay Soil*, Journal of Engineering, **5**(5), 2011.

[9] Zhenghu, H.Z, Zianhui, H.D. & Jianbo, B.Z., *A Rapid and Nondestructive Method to Determine Normal and Shear Stiffness of a Single Rock Joint Based on 1D Wave-propagation Theory*, Geophysics, **83**(1), pp. 1-12, 2018.

[10] Ohsaki, Y. & Iwasaki, R., *On Dynamic Shear Moduli and Poisson's Ratio of Soil Deposits*, Soils and Foundations, **13**(4), pp. 59-73, 1973.

[11] Ohta, Y. & Goto, N., *Empirical Shear Wave Velocity Equations in Terms of Characteristic Soil Indexes*, Earthquake Engineering and Structural Dynamics, **6**, pp. 167-187, 1978.

[12] Imai, T. & Tonouchi, K., *Correlation of N Value with S-wave Velocity and Shear Modulus*, Second European Symposium on Penetration Testing, Amsterdam, The Netherlands, pp. 67-72, 1982.

[13] Maheswari, U. R., Boominathan, A. & Dodagoudar, G. R. *Development of Empirical Correlation Between Shear Wave Velocity and Standard Penetration Resistance in Soils of Chennai City*, 14th World Conference on Earthquake Engineering, Beijing, China, 2008.

[14] Dikmen, U., *Statistical Correlations of Shear Wave Velocity and Penetration Resistance for Soils*, Journal of Geophysics and Engineering, **6**, pp. 61-72, 2009.

[15] Partono, W., Wardani S.P.R., Irsyam M. and Maarif S., *Development of Seismic Microzonation Maps of Semarang, Indonesia*, Jurnal Teknologi, **77**(11), pp. 99-107, 2015.

Site Soil Classification Interpretation Based on Standard Penetration Test and Shear Wave Velocity Data

ORIGINALITY REPORT

7%	4%	5%	1%
SIMILARITY INDEX	INTERNET SOURCES	PUBLICATIONS	STUDENT PAPERS

PRIMARY SOURCES

1	geomatejournal.com Internet Source	1%
2	W Partono, F Kistiani, U C Sari, Haryadi, E Putro, W R Ramadhan. "Development of surface ground motion and spectral acceleration based on modified shear wave propagation analysis", IOP Conference Series: Materials Science and Engineering, 2019 Publication	1%
3	Windu Partono, Masyhur Irsyam, Sri Prabandiyani Retno Wardani. "Development of site class and site coefficient maps of Semarang, Indonesia using field shear wave velocity data", MATEC Web of Conferences, 2017 Publication	<1%
4	Submitted to Universitas Diponegoro Student Paper	<1%
5	eprints.undip.ac.id Internet Source	<1%

6	Submitted to School of Business and Management ITB Student Paper	<1%
7	eprints.usm.my Internet Source	<1%
8	Abhishek Kumar, P. Anbazhagan, T. G. Sitharam. "Liquefaction Hazard Mapping of Lucknow", International Journal of Geotechnical Earthquake Engineering, 2013 Publication	<1%
9	Windu Partono, Yulita Ami Priastiwi, Nuroji, Indrastono Dwi Atmanto et al. "Structural analysis using three-component acceleration time histories caused by shallow crustal fault earthquakes with a maximum magnitude of 7 Mw", MATEC Web of Conferences, 2019 Publication	<1%
10	www.wit.uni-hamburg.de Internet Source	<1%
11	Ümit Gülerce. "Comment on 'Statistical correlations of shear wave velocity and penetration resistance for soils'", Journal of Geophysics and Engineering, 03/01/2010 Publication	<1%
12	Submitted to University of Newcastle upon Tyne Student Paper	<1%

13	Li Wu, Johan Tordsson, Jasmin Bogatinovski, Erik Elmroth, Odej Kao. "MicroDiag: Fine-grained Performance Diagnosis for Microservice Systems", 2021 IEEE/ACM International Workshop on Cloud Intelligence (CloudIntelligence), 2021 Publication	<1 %
14	Windu Partono, Masyhur Irsyam, Sri Prabandiyani Retno Wardani. "Development of acceleration time histories for Semarang, Indonesia, due to shallow crustal fault earthquakes", AIP Publishing, 2017 Publication	<1 %
15	"Proceedings of the Indian Geotechnical Conference 2019", Springer Science and Business Media LLC, 2021 Publication	<1 %
16	Gökçe Çiçek İnce. "Seismic microzonation of the historic peninsula of İstanbul", Bulletin of Engineering Geology and the Environment, 02/2008 Publication	<1 %
17	Odgers, Nathan P., Wei Sun, Alex B. McBratney, Budiman Minasny, and David Clifford. "Disaggregating and harmonising soil map units through resampled classification trees", Geoderma, 2013. Publication	<1 %

18	P. Anbazhagan. "Seismic microzonation of Bangalore, India", Journal of Earth System Science, 11/2008 Publication	<1 %
19	Samuel D. Crish, Frank L. Rice, Thomas J. Park, Christopher M. Comer. "Somatosensory Organization and Behavior in Naked Mole-Rats I: Vibrissa-Like Body Hairs Comprise a Sensory Array That Mediates Orientation to Tactile Stimuli", Brain, Behavior and Evolution, 2003 Publication	<1 %
20	Windu Partono, Bambang Pardoyo, Indrastono Dwi Atmanto, Lisa Azizah, Rouli Dian Chintami. "Sensitivity analysis of tall buildings in Semarang, Indonesia due to fault earthquakes with maximum 7 Mw", AIP Publishing, 2017 Publication	<1 %
21	assets.researchsquare.com Internet Source	<1 %
22	www.ncbi.nlm.nih.gov Internet Source	<1 %

Exclude quotes	Off	Exclude matches	Off
Exclude bibliography	On		